Communication

High-Speed Spiral-Phase Donut-Modes-Based Hybrid FSO-MMF Communication System by Incorporating OCDMA Scheme

Meet Kumari [1] **, Abhishek Sharma** [2] **and Sushank Chaudhary** [3,*]

[1] Department of Electronics and Communication Engineering, Chandigarh University,
    Mohali 140413, Punjab, India
[2] Department of Electronics Technology, Guru Nanak Dev University, Amritsar 143005, Punjab, India
[3] Department of Electrical Engineering, Chulalongkorn University, Bangkok 10330, Thailand
[*] Correspondence: sushankchaudhary@gmail.com

Abstract: Hybrid free-space optics (FSO) and optical fiber have been viewed as vital transmission techniques to satisfy high bandwidth and extended transmission range requirements under adverse environment conditions in the future last-mile obstruction problem. In this investigation, 80 Gbps data is transmitted on a hybrid FSO and multimode fiber (MMF)-based network using mode division multiplexing of two donut modes, Donut mode 0 and 1, and optical code-division multiplexing (OCDMA) schemes. For the OCDMA schemes, modified new zero-cross-correlation (MNZCC) codes are used, whereas, to add the phases into donut modes, a spiral phase diffuser is used. The purpose of the investigation is to provide an economical, high-speed and advanced last-mile network with adequate resource utilization for hybrid wired/wireless-based systems. The results obtained show achievement of an acceptable BER up to a fixed 100 m FSO link, with the combination of a 385 m MMF link under clear weather conditions. In another case, when the MMF link was fixed at 100 m, an acceptable bit error rate (BER) is achieved at 2.07 km FSO link. Furthermore, the results were obtained in the presence of strong and weak turbulences. A comparison of log-normal and gamma-gamma modeling for scintillations is presented.

Keywords: donut modes; free-space optics (FSO); mode-division multiplexing (MDM); optical code division multiple access (OCDMA)

1. Introduction

The last few years have seen a considerable increase in data traffic owing to growth in the use of multimedia applications which utilize high channel bandwidth, such as video conferencing, live streaming and fast internet, which has challenged the congested and limited radio-frequency-spectrum-based traditional wireless transmission networks. Free-space optics (FSO) can be regarded as a favorable solution with the purpose of achieving the high capacity and high transmission rates desired by end-users [1,2]. Optically modulated signals are utilized to transport traffic signals over the wireless medium between aligned transmitters along with receiver units. The FSO mechanism offers several advantages, including quick and easy installation, electromagnetic interference immunity, high channel bandwidth, secure information transmission, high-speed transmission, a license-free spectrum and cost-effective communication availability [3]. Optical code-division multiple access (OCDMA) is used in optical communication networks for merging distant data types with enhanced bandwidth by using codes [4,5]. However, OCDMA performance is affected by the rising number of subscribers due to multiple access interference (MAI). This shortcoming can diminish the effectiveness of OCDMA systems and, to minimize its effect, an optimum code sequence and detection technique needs to be implemented appropriately. As an efficient and secure system, OCDMA is used extensively in wireless

systems. OCDMA has attracted significant attention for its capacity to enhance bandwidth demand, making it appropriate for designing cross-correlated code patterns to distinguish interfacing and intended signals [5]. Moreover, the optical code, as well as the coding arrangement, needs to be suitable for the provision of quality network services.

Recently, researchers have presented several codes for spectral-amplitude coding (SAC)-based OCDMA systems, including optical orthogonal [6], random diagonal (RD) [7], modified frequency hopping (MFH) [8], modified double-weight (MDW) [9], multi-diagonal (MD) [10] codes and others. On the other hand, optical networks use mode-division multiplexing (MDM) to enhance system capacity through multimode channel transmission over a single wavelength, which can efficiently resolve bandwidth and spectrum issues [11]. An MDM-integrated hybrid OCDMA-FSO system was used to improve system capacity and to reduce MAI effects in [12]. In [3], a hybrid orthogonal frequency-division multiplexing (OFDM) FSO link system using a Hermite-Gaussian (HG)-modes-based wavelength MDM scheme over 32 km at 80 Gbps under different weather conditions is described. In [12], an HG-modes MDM-based OCDMA system using RD code over an 11 km multimode link at a 100 Gbps data rate was presented. In [13], the authors proposed a hybrid MDM-OCDM system using linearly polarized (LP) modes, which was able to transmit 80 Gbps data over a 2 km two-mode fiber. In [14], a Laguerre–Gaussian (LG)-modes MDM-FSO system, using SZCC and MD codes over 12 and 10 km, respectively, at 100 Gbps for 10 users was described. In [15], a hybrid LP-modes MDM code-division multiplexing (CDM)-based transmission system, which supported transmission of 80 Gbps over a 42 km fiber distance, was proposed. In [16], an LP-modes MDM-OCDMA-PON system with transmission over 40 km single-mode fiber and 2 km two-mode fiber (TMF) at a 80 Gbps data rate was proposed. In [8], a hybrid MDM-FSO-OCDMA system with a 100 Gbps transmission rate over an 8 km FSO range, under adverse environment conditions, was proposed. In [17], a 40 Gbps MDM-based radio-over-FSO (Ro-FSO) using LG and HG modes over a 50 km transmission distance was described. In [18], the design of a hybrid LG-modes MDM-OCDMA-FSO system operating at 120 Gbps, using an identity-type matrix ZCC over 1.750 km, was reported. In [19], the authors demonstrated an MDM-based PON-FSO using LG modes over a 155 km multimode fiber and a 1000 m FSO. In [20], a hybrid FSO-WDM-PON system, with four and two downstream and upstream channels, respectively, transmitting at a 10 Gbps data rate over a 60 km SMF and a 650 m FSO range, was presented. In [21], a PON-FSO system using an MNZCC code over a 10 km SMF and a 500 m FSO range at a 10/2.5 Gbps data rate was described.

In this investigation, an MDM-OCDMA-based transmission system is demonstrated, which uses mode multiplexing of Donut modes 0 and 1 to transmit 80 Gbps of data over a hybrid FSO and MMF transmission link. An MNZCC code is used to reduce the MAI effect and to enhance the system security with eight input channels. The performance of the link was measured in terms of the bit error rate (BER) under clear weather conditions, as well as under strong, medium and weak turbulences. The rest of the paper is organized as follows: Section 2 presents the modeling of the proposed MDM-OCDMA-FSO system. The results and discussion are presented in Section 3, and the conclusions in Section 4.

2. Modeling of MDM-OCDMA System

Figure 1 depicts a block diagram of the proposed 8 × 10 Gbps MDM-based FSO-OCDMA system by incorporating MNZCC code.

The proposed OCDMA-MDM-FSO-MMF model is modeled in OptiSystem^{TM} V-19 and Matlab^{TM} due to their high accuracy. In the proposed OCDMA-based MDM-FSO-MMF system, there are eight channels with a group of four channels operating at four MNZCC code sequences for four users. At the transmitter side, two external continuous wave (CW) laser arrays with an input power of 10 dBm are used. Here, each CW laser array generates twelve wavelengths of 1550, 1551.6, 1552.4, 1553.2, 1554, 1554.8, 1555.6, 1556.4, 1555.6, 1557.2, 1558 and 1558.8 nm, as depicted in Figure 1a. In each transmitter, a 12:1 ideal multiplexer multiplexes all input signals and transfers them to the 1:12 wavelength-division

multiplexing (WDM) demultiplexer. Each encoder consists of a 3:1 WDM multiplexer to multiplex different input wavelengths as per the MNZCC code sequence, PRBS, to generate a random bit sequence, NRZ pulse generator and Mach–Zehnder modulator (MZM) to modulate the coded signals. A 4:1 ideal multiplexer is used to multiplex the outputs of distinct coded signals representing four transmission channels. The output of the multiplexer is fed to a donut mode generator which generates the Donut mode 0. Similarly, in another transmitter, the next four transmission channels are fed to a donut mode generator which generates the Donut mode 1. The generated donut modes are shown in Figure 2. A 2:1 power combiner is used to combine the incoming signals operating at two different modes for propagation through the FSO link, followed by a multimode fiber, as shown in Figure 1b.
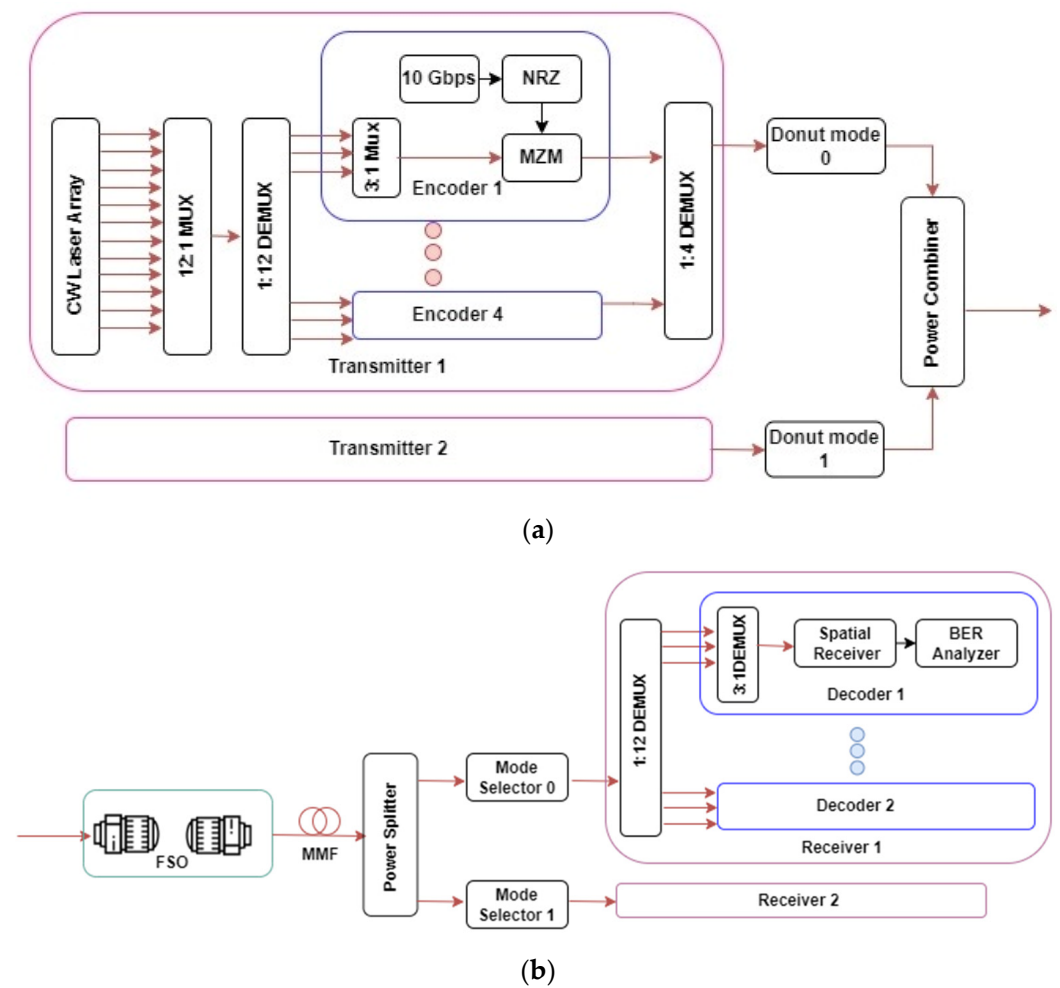

(**a**)

(**b**)

Figure 1. Proposed 8 × 10 Gbps OCDMA based MDM-FSO-MMF system of (**a**) transmitter, (**b**) receiver.

At the receiver side, a splitter is used to split the optical signal into two parts; each one is followed by the mode selector, which selects the desired mode transmitted on the transmitter side. The output of the mode selector is fed to the relevant receiver side which consists of four decoders to decode the output for four end users. A decoder consists of a 3:1 WDM multiplexer followed by a spatial optical receiver to recover the original baseband signal, followed by a low-pass filter (LPF). Tables 1 and 2 present the MNZCC code design used in the system for four users at Donut mode 0 and 1, respectively. Table 3 shows the various parameters used in the modeling of the proposed system.
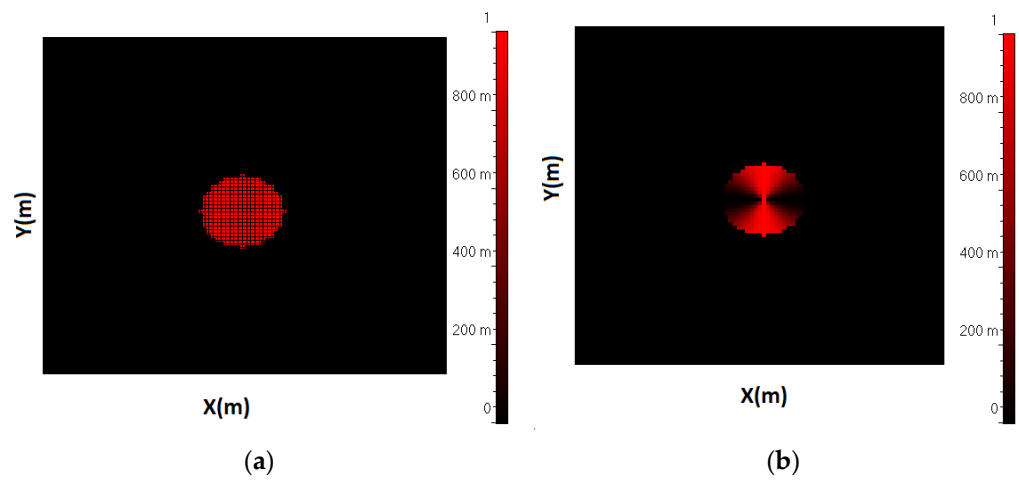
Figure 2. Generated donut modes. (**a**) Donut mode 0, (**b**) Donut mode 1.

Table 1. MNZCC code design for four users at Donut mode 0.

Wavelength (nm)	1550	1550.8	1551.6	1552.4	1553.2	1554	1554.8	1555.6	1556.4	1557.2	1558	1558.8
User 1	1	0	0	0	1	0	0	0	1	0	0	0
User 2	0	1	0	0	0	1	0	0	0	1	0	0
User 3	0	0	1	0	0	0	1	0	0	0	1	0
User 4	0	0	0	1	0	0	0	1	0	0	0	1

Table 2. MNZCC code design for four users at Donut mode 1.

Wavelength (nm)	1550	1550.8	1551.6	1552.4	1553.2	1554	1554.8	1555.6	1556.4	1557.2	1558	1558.8
User 1	1	0	0	0	1	0	0	0	1	0	0	0
User 2	0	1	0	0	0	1	0	0	0	1	0	0
User 3	0	0	1	0	0	0	1	0	0	0	1	0
User 4	0	0	0	1	0	0	0	1	0	0	0	1

Table 3. Parameter values for MDM-based FSO-OCDMA system.

Parameters	Values
Laser input power	10 dBm
Wavelength	1550–1558.8 nm
Data rate	10 Gbps
Tx aperture diameter	15 cm
Rx aperture diameter	20 cm
Reference wavelength	1550 nm
Dark current	10 nA
FSO range	1500–2200 m
Measured index multimode fiber length	320–420 m
Mux/De-mux bandwidth	10 GHz
Mux/De-mux filter type	Bessel
Mux/De-mux filter order	2
MZM extinction ratio	30 dB
NRZ rectangle shape	Exponential
NRZ amplitude	1 a.u.
Turbulence condition	Weak (10^{-17} m$^{-2/3}$) and strong (10^{-13} m$^{-2/3}$)
Turbulence model	Gamma-Gamma and log-normal

3. Results and Discussion

In this section, the results from the modeling of the proposed MDM-OCDMA-FSO system using MNZCC code are presented and discussed under different scintillation effects and clear air weather conditions using OptiSystem v.19 simulation software. We considered two cases for the transmission link. In the first case, the FSO range was fixed at 100 m, whereas the multimode fiber length was varied from 320 m to 420 m. In another case, the MMF range was fixed at 100 m and the FSO range was varied from 1.5 to 2.2 km. Figure 3 presents the BER performance of the proposed MDM-OCDMA-FSO system under clear weather conditions. The scintillation is considered ideal in this case.
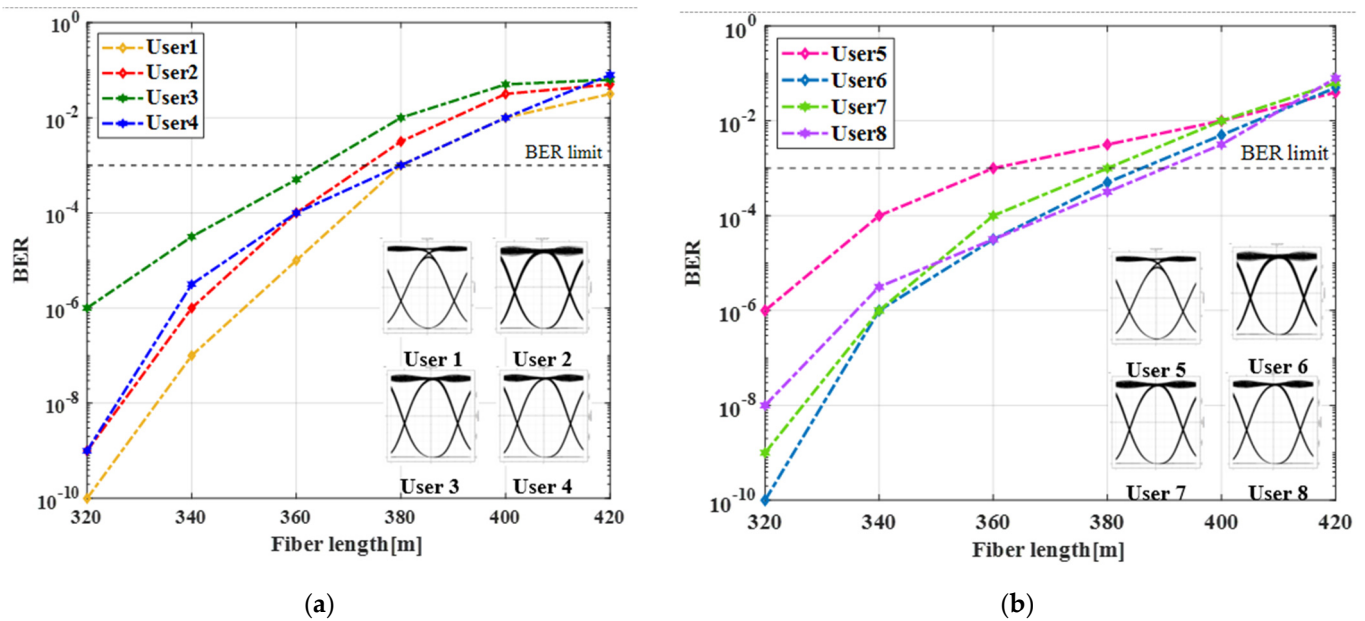

Figure 3. Measured BER at fixed FSO link of 100 m under clear air conditions. (**a**) Users 1 to 4 operating on Donut mode 0 and with corresponding eye patterns at 320 m fiber length, (**b**) users 5 to 8 operating on Donut mode 1 with corresponding eye patterns at 320 m fiber length.

With increase in fiber length, the BER value increases and, hence, the system performance decreases for all users. User 1, User 2, User 3 and User 4 achieve a BER of less than 10^{-3} at the MMF lengths of 380, 375, 365 and 380 m, respectively, for Donut mode 0, as shown in Figure 3a. Similarly, for Users 5 to 8 operating on Donut mode 1, an acceptable BER 10^{-3} is achieved for User 5, User 6, User 7 and User 8 at the fiber lengths of 360, 385, 380 and 390 m, respectively, as shown in Figure 3b. The measured eye spectrums at 320 m fiber length show the successful transmission of all the users. Further, it is observed that performance of the hybrid fiber-FSO link is restricted due to the presence of fiber non-linearities and noise. Thus, the obtained faithful MMF fiber range is 380 m with a 100 m FSO range, in the presence of fiber interference and an FSO weak turbulence effect.

Figure 4 shows the measured BER plots where the MMF length is fixed at 100 m and the FSO range is varied. The figure shows that User 1, User 2, User 3 and User 4 achieve a BER of less than 10^{-3} at the MMF lengths of 2.05 km, 2.07 km, 2.10 km and 2 km, respectively, as shown in Figure 3a. Similarly, as shown in Figure 3b, an acceptable BER of 10^{-3} is achieved for User 5, User 6, User 7 and User 8 at FSO ranges of approximately 2.05 km, 2.07 km, 1.95 km and 1.9 km. From Figures 3 and 4, it can be seen that users which are operated on Donut mode 0 achieve good BER compared to users which are operated on Donut mode 1. Furthermore, the performance of the proposed OCDMA-based MDM-FSO-MMF was also investigated under the impact of scintillations. It is shown that the performance of the hybrid fiber-FSO link is limited due to the presence of FSO channel interference and turbulence effects. Therefore, the maximum achieved FSO range

is 2.10 km with 100 m MMF fiber, in the presence of fiber interference and an FSO weak turbulence effect.
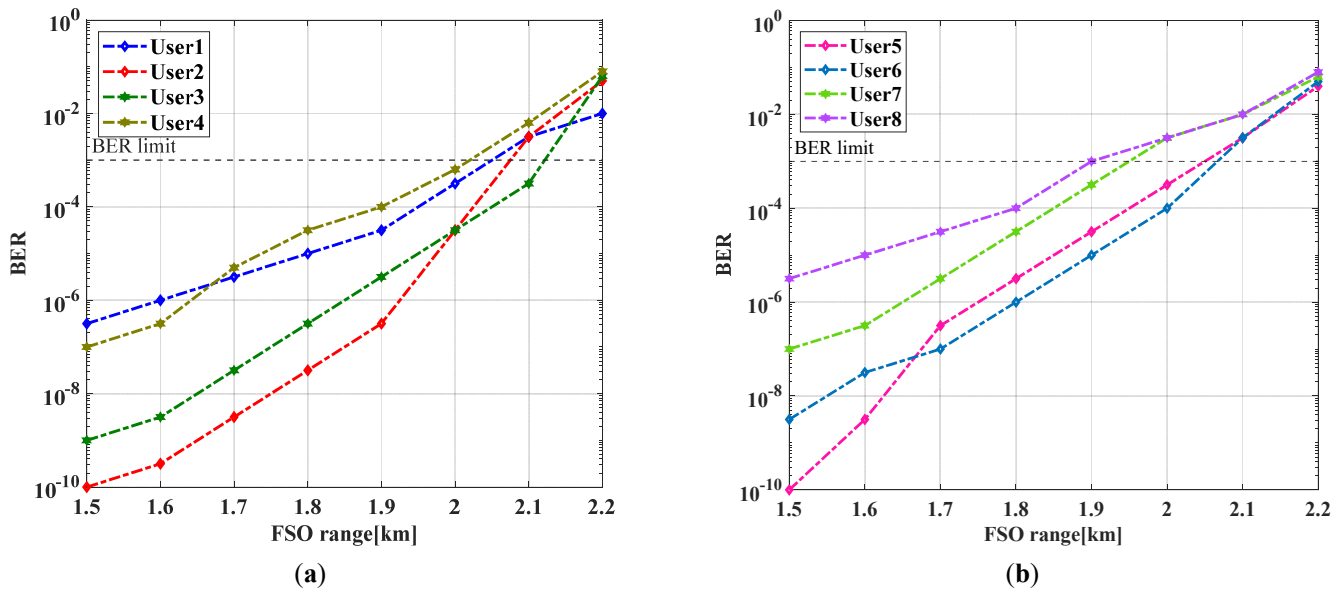

Figure 4. Measured BER at fixed MMF link of 100 m under clear air conditions. (**a**) Users 1 to 4 operating on Donut mode 0, (**b**) users 5 to 8 operating on Donut mode 1.

For the impact of scintillations, both gamma-gamma and log-normal modeling are considered. In the case of gamma-gamma modeling, Figure 5a,b present the BER performance of the proposed OCDMA-based MDM-FSO-MMF system using MNZCC code over a fixed 300 m fiber along with a variable FSO range. Eight users at Donut mode 0 and Donut mode 1 under both weak (10^{-17} m$^{-2/3}$) and strong turbulences (10^{-13} m$^{-2/3}$) are considered. It can be seen that, as the atmospheric turbulence strength increases, the BER values again increase over a varied FSO range from 700–2100 m. The figure also shows that User 1 and User 5 in the system at Donut mode 0 and 1, respectively, exhibit the best performance out of all eight users under both weak and strong turbulences. The value of an acceptable BER ($\leq 10^{-3}$) is computed for User 1, User 2, User 3 and User 4 under the impact of weak turbulences at the FSO transmission ranges of 2100, 1800, 1900 and 1500 m, respectively. Similarly, under the impact of strong turbulences, an acceptable BER ($\leq 10^{-3}$) is computed for User 1, User 2, User 3 and User 4 at the FSO transmission ranges of 1720, 1600, 1520 and 1150 m, respectively.

For User 5, User 6, User 7 and User 8 under the impact of weak turbulences, an acceptable BER ($\leq 10^{-3}$) is achieved at FSO transmission ranges of 2100, 1500, 1700 and 1300 m respectively, as shown in Figure 4b. However, the maximum FSO ranges under strong turbulence for User 5, User 6, User 7 and User 8 are 1150, 1000, 700 and 800 m, respectively.

Figure 6a,b presents the BER performance of the proposed OCDMA-based MDM-FSO-MMF system over a fixed 300 m fiber along with a variable FSO range employing a log-normal turbulence model. The figure shows that the value of an acceptable BER for User 1, User 2, User 3 and User 4 under the impact of weak turbulences is achieved at the FSO transmission distances of 2100, 1800, 1900 and 1500 m, respectively. On the other hand, under the impact of strong turbulences, the required BER is computed for the User 5, User 6, User 7 and User 8 at the FSO ranges of 1800, 1600, 1250 and 1150 m, respectively. Thus, it is observed that the gamma-gamma model shows better performance than the log-normal turbulence model as the former can perform more effectively under correlation as opposed to other fading channel models.
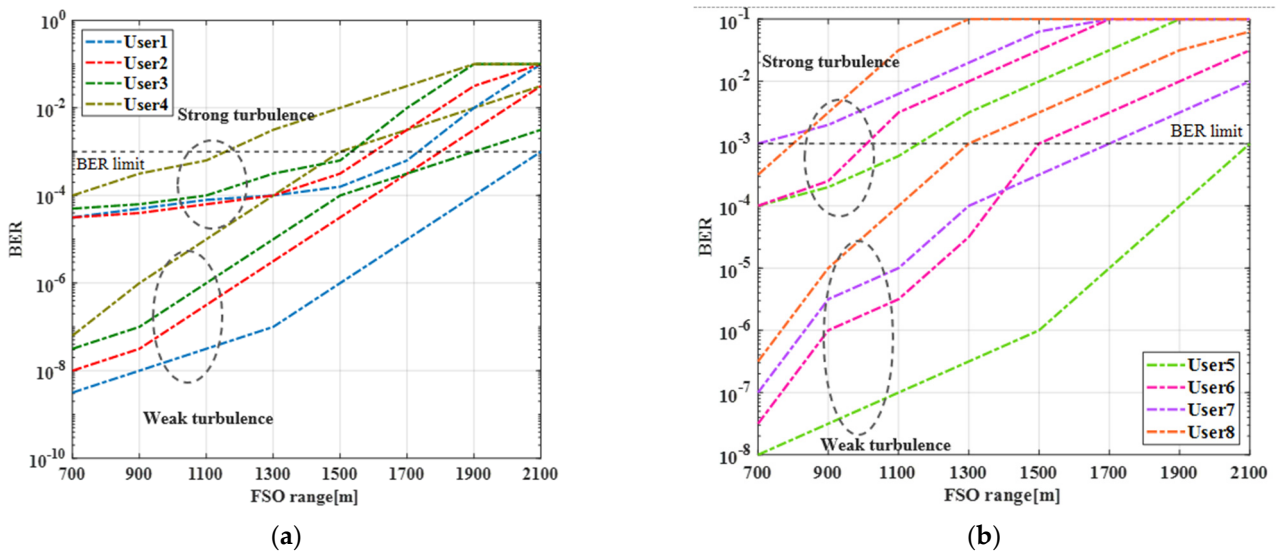
Figure 5. Measured BER under gamma-gamma turbulence modeling. (**a**) Users 1 to 4 operating at Donut mode 0, (**b**) users 5 to 8 operating at Donut mode 1.
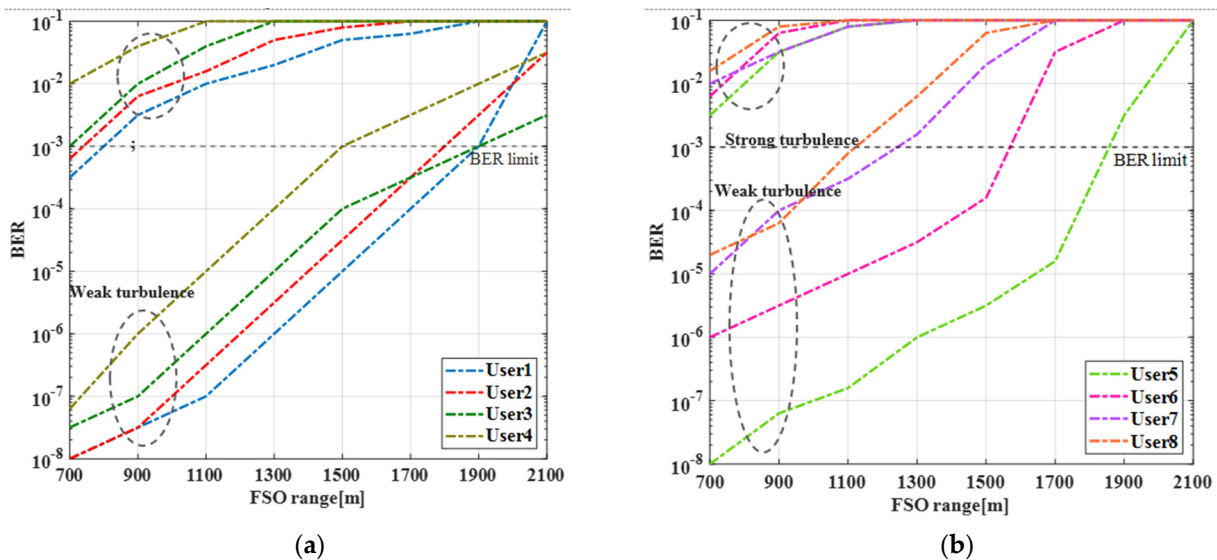

Figure 6. Measured BER under log-normal turbulence modeling. (**a**) Users 1 to 4 operating at Donut mode 0, (**b**) users 5 to 8 operating at Donut mode 1.

4. Conclusions

In this investigation, an 8 × 10 Gbps OCDMA-based hybrid MDM-FSO-MMF system was designed by incorporating MNZCC code. To design the MDM scheme, modal multiplexing of Donut modes 0 and 1 was used. Users that were transmitted on Donut mode 0 performed slightly better compared to users that were transmitted on Donut mode 1, as the latter suffered more from attenuation. For an acceptable/required BER, the maximum achieved MMF was 385 m with a 100 m FSO range under clear air climate conditions. Moreover, when the MMF was fixed at 100 m, the FSO range could be extended up to 2.07 km. Furthermore, the effect of scintillations, particularly weak and strong turbulences, on the performance of the proposed OCDMA-based MDM-FSO-MMF model was investigated. The results show that for both gamma-gamma and log-normal modeling, all the users transmitted on Donut mode 0 and Donut mode 1 achieved acceptable BER values up to 1150 m. Therefore, the OCDMA-based hybrid MDM-FSO-MMF system can improve the usage of an FSO-fiber link under different atmospheric conditions. The proposed system

can offer high data-rate and long-range hybrid wired-wireless link services under adverse environment conditions in the future.

References

1. Le, H.D.; Pham, A.T. Link-Layer Retransmission-Based Error-Control Protocols in FSO Communications: A Survey. *IEEE Commun. Surv. Tutor.* **2022**, *24*, 1602–1633. [CrossRef]
2. Mohsan, S.A.H.; Khan, M.A.; Amjad, H. Hybrid FSO/RF Networks: A Review of Practical Constraints, Applications and Challenges. *Opt. Switch. Netw.* **2023**, *47*, 100697. [CrossRef]
3. Singh, M.; Chebaane, S.; Ben Khalifa, S.; Grover, A.; Dewra, S.; Angurala, M. Performance Evaluation of a 4 × 20-Gbps OFDM-Based FSO Link Incorporating Hybrid W-MDM Techniques. *Front. Phys.* **2021**, *9*, 460. [CrossRef]
4. Mohammed, H.A.; Abu Bakar, M.H.; Anas, S.B.A.; Mahdi, M.A.; Yaacob, M.H. Optical Fiber Sensor Network Integrating SAC-OCDMA and Cladding Modified Optical Fiber Sensors Coated with Nanomaterial. *Opt. Fiber Technol.* **2022**, *70*, 102875. [CrossRef]
5. Mrabet, H.; Cherifi, A.; Raddo, T.; Dayoub, I.; Haxha, S. A Comparative Study of Asynchronous and Synchronous OCDMA Systems. *IEEE Syst. J.* **2021**, *15*, 3642–3653. [CrossRef]
6. Ortiz-Ubarri, J. New Asymptotically Optimal Three-Dimensional Wave-Length/Space/Time Optical Orthogonal Codes for OCDMA Systems. *Cryptogr. Commun.* **2020**, *12*, 785–794. [CrossRef]
7. Kumawat, S.; Kumar, M.R. A Review on Code Families for SAC—OCDMA Systems. In *Optical and Wireless Technologies*; Springer: Berlin/Heidelberg, Germany, 2020; pp. 307–315.
8. Sarangal, H.; Singh, A.; Malhotra, J.; Chaudhary, S. A Cost Effective 100 Gbps Hybrid MDM–OCDMA–FSO Transmission System under Atmospheric Turbulences. *Opt. Quantum Electron.* **2017**, *49*, 184. [CrossRef]
9. Ahmed, N.; Aljunid, S.A.; Fadil, A.; Ahmad, R.B.; Rashid, M.A. Performance Enhancement of OCDMA System Using NAND Detection with Modified Double Weight (MDW) Code for Optical Access Network. *Opt. Int. J. Light Electron. Opt.* **2013**, *124*, 1402–1407. [CrossRef]
10. Jellali, N.; Najjar, M.; Ferchichi, M.; Rezig, H. Three-Dimensional Multi-Diagonal Codes for OCDMA System. *Optik* **2017**, *145*, 428–435. [CrossRef]
11. Su, Y.; He, Y.; Chen, H.; Li, X.; Li, G. Perspective on Mode-Division Multiplexing. *Appl. Phys. Lett.* **2021**, *118*, 200502. [CrossRef]
12. Upadhyay, K.K.; Shukla, N.K.; Chaudhary, S. A High Speed 100 Gbps MDM-SAC-OCDMA Multimode Transmission System for Short Haul Communication. *Optik* **2020**, *202*, 163665. [CrossRef]
13. Kodama, T.; Isoda, T.; Morita, K.; Maruta, A.; Maruyama, R.; Kuwaki, N.; Matsuo, S.; Wada, N.; Cincotti, G.; Kitayama, K. Hybrid MDM/OCDM System with Mode and Code Multi-/Demultiplexers. In Proceedings of the SPIE-Next-Generation Optical Communication: Components, Sub-Systems, and Systems III, San Francisco, CA, USA, 1 February 2014; Volume 9009, pp. 124–130.
14. Kaur, R.; Singh, K. Performance Analysis of Shift ZCC Codes and Multi Diagonal Codes in 100 Gbps MDM-FSO System. *J. Opt. Commun.* **2020**. [CrossRef]
15. Kodama, T.; Isoda, T.; Morita, K.; Maruta, A.; Maruyama, R.; Kuwaki, N.; Matsuo, S.; Wada, N.; Cincotti, G.; Kitayama, K. First Demonstration of a Scalable MDM/CDM Optical Access System. *Opt. Express* **2014**, *22*, 12060–12069. [CrossRef] [PubMed]
16. Kodama, T.; Isoda, T.; Morita, K.; Maruta, A.; Maruyama, R.; Kuwaki, N.; Matsuo, S.; Wada, N.; Cincotti, G.; Kitayama, K.I. Asynchronous MDM-OCDM-Based 10G-PON over 40km-SMF and 2km-TMF Using Mode MUX/DeMUX at Remote Node and OLT. In Proceedings of the Optical Fiber Communication Conference, OFC, Los Angeles, CA, USA, 9–14 March 2014; p. W2A-9.
17. Chaudhary, S.; Lin, B.; Tang, X.; Wei, X.; Zhou, Z.; Lin, C.; Zhang, M.; Zhang, H. 40 Gbps–80 GHz PSK-MDM Based Ro-FSO Transmission System. *Opt. Quantum Electron.* **2018**, *50*, 321. [CrossRef]
18. Sarangal, H.; Nisar, K.S.; Thapar, S.S.; Singh, A.; Malhotra, J. Performance Evaluation of 120 GB/s Hybrid FSO-SACOCDMA-MDM System Using Newly Designed ITM-Zero Cross-Correlation Code. *Opt. Quantum Electron.* **2021**, *53*, 64. [CrossRef]

19. Kumari, M.; Sharma, R.; Sheetal, A. Performance Analysis of Long-Reach 40/40 Gbps Mode Division Multiplexing-Based Hybrid Time and Wavelength Division Multiplexing Passive Optical Network/Free-Space Optics Using Gamma-Gamma Fading Model with Pointing Error under Different Weather Conditions. *Trans. Emerg. Telecommun. Technol.* **2021**, *32*, e4214. [CrossRef]

20. Mandal, P.; Sarkar, N.; Santra, S.; Dutta, B.; Kuiri, B.; Mallick, K.; Patra, A.S. Hybrid WDM-FSO-PON with Integrated SMF/FSO Link for Transportation of Rayleigh Backscattering Noise Mitigated Wired/Wireless Information in Long-Reach. *Opt. Commun.* **2022**, *507*, 127594. [CrossRef]

21. Kumari, M.; Arya, V. Investigation of High-Speed Hybrid WDM-OCDMA-PON System Incorporating Integrated Fiber-FSO Link under Distinct Climate Conditions. *Opt. Quantum Electron.* **2022**, *54*, e4699. [CrossRef]